PHYSICAL REVIEW D **94,** 025037 (2016)

Multi-Skyrmions with orientational moduli

F. Canfora[1,*] and G. Tallarita[2,†]

[1]*Centro de Estudios Científicos (CECS), Casilla 1469, Valdivia, Chile*

[2]*Departamento de Ciencias, Facultad de Artes Liberales, Universidad Adolfo Ibáñez, Santiago 7941169, Chile*

(Received 27 May 2016; published 28 July 2016)

We analyze the mechanism of condensation of orientational moduli [as introduced in Phys. Rev. D **87**, 025025 (2013)] on multi-Skyrmionic configurations of the four-dimensional Skyrme model. The present analysis reveals interesting novel features. First of all, the orientational moduli tend to decrease the repulsive interactions between Skyrmions, the effect decreasing with the increase of the baryon number. Moreover, in the case of a single Skyrmion, the appearance of moduli is energetically favorable if finite-volume effects are present. Otherwise, in the usual flat topologically trivial case, it is not. In the low-energy theory these solutions can be interpreted as Skyrmions with additional isospin degrees of freedom.

DOI: 10.1103/PhysRevD.94.025037

I. INTRODUCTION

Skyrme's theory [1] is one of the most important models in theoretical physics due to its wide range of applications in the low-energy limit of QCD (for a nice review, see [2]). Skyrme included his famous term into the action of the four-dimensional nonlinear sigma model to allow the existence of static soliton solutions with finite energy, called Skyrmions. A quite remarkable feature of this construction is that the Skyrmion represents a fermionic degree of freedom suitable to describe a baryon. This very deep intuition together with the close relation between low-energy QCD and the Skyrme model itself were rigorously proved in the classic papers [3–5]. Moreover, from the quantitative point of view, the theoretical and numerical computations based on the Skyrme model are in good agreement with the experimental data in nuclear physics [6–10].

Unfortunately, unlike what happens for instance in the case of monopoles and instantons in Yang-Mills-Higgs theory (see [2]), it is extremely difficult to construct exact nontrivial solutions of the Skyrme field equations in which the nonlinear effects of the Skyrme term are manifest. The reason is that on flat topologically trivial space-times, the BPS bound on the energy in terms of the baryon number (which was derived by Skyrme himself) cannot be saturated for spherically symmetric Skyrmions. Thus, until very recently, basically no exact nontrivial solution of the four-dimensional Skyrme model was available. Even less exact results are available in all the situations in which Skyrmions are confined to live within a finite volume/density (see, for instance, the analysis of [11]). In many of the applications of the Skyrme model in nuclear physics and astrophysics one expects finite-volume effects to be relevant, but, of course, such effects usually make matters worse in terms of finding exact solutions (as, for instance, finite-volume effects break the symmetries of the most common *Ansatz*).

Using the formalism developed in [12,13], the first exact solutions of the four-dimensional $SU(2)$ Skyrme model in which the nonlinear effects of the Skyrme term are manifest have been constructed in [14]. Such solutions may possess nontrivial topological charges different from the baryon number. The conclusions of [14] have been strengthened in [15]. Using these results, in [16] the first exact multi-Skyrmionic solutions of arbitrary baryon number, living within a finite volume and composed of interacting elementary $SU(2)$ Skyrmions, have been constructed. The useful mathematical trick to construct these configurations has been to place them within a suitable tube-shaped finite-volume space-time (which, in the context of the Skyrme model, has been also considered in [17], though with different motivations). The main role of this topology is to maintain the finite-volume effects without breaking the symmetries of the *Ansatz*. The quite nontrivial technical advantage of this choice to describe finite-volume effects is that it allows us to compute explicitly the Skyrmion-Skyrmion interaction energy. This computation shows clearly the repulsive character of Skyrmion-Skyrmion interactions within this tube-shaped region. These results have been generalized in [18] for the $SU(N)$ case. Moreover, these results allowed the first analytic construction of gravitating Skyrmions in [19].

This framework offers the intriguing possibility to analyze a very important phenomenon which is typical of many topological defects: the condensation of additional orientational moduli on their world sheet (in the case of Skyrmions, world line). These orientational moduli are simply the Goldstone bosons which arise by breaking a non-Abelian global symmetry on the core of the original solitons. The corresponding solutions are called non-Abelian solitons. The case of non-Abelian vortices has

*canfora@cecs.cl

†gianni.tallarita@uai.cl

been of particular interest as a possible description of the vortices responsible for the dual [20] confinement of quarks in QCD. Research in this direction, pioneered by [21–24], led Shifman to develop a particularly simple model (inspired by the famous Witten result on superconducting cosmic strings [25]) in which orientational moduli can condense on solitonic solutions [26]. The model was recently used to construct the first case of non-Abelian vortices in holographic models at strong coupling [27]. The analysis shows that the main ingredients responsible for the presence of orientational moduli are (i) a bulk theory with a global non-Abelian symmetry G (which must be unbroken initially) and which admits topological defects uncharged under this symmetry (Skyrmions in the present case) and (ii) the breaking of G down to a global subgroup H on the given defect. The orientational moduli are then the Goldstone bosons of the symmetry breaking pattern $G \to H$ and their low-energy dynamics is described by the nonlinear sigma model with target space G/H.

In this paper we will adapt this model to produce Skyrmions with orientational moduli. Given the previous results on multi-Skyrmion solutions we are able to extend this study to the case of multisolitonic configurations. In particular this allows us to infer some characteristics of the moduli interactions, of which little is known (see for example [28]), and to study their finite-volume physics. In fact, most of the previously known applications of [26] dealt with moduli localized on isolated topological soliton (for example see [29–32]). This analysis reveals many interesting novel features. First of all, the orientational moduli of [26], when finite-volume effects are taken into account as in [16], tend to decrease the repulsive interactions among Skyrmions which characterize the multi-Skyrmionic configurations living in the tube-shaped regions mentioned above. Moreover the appearance of moduli is energetically favorable if finite-volume effects are present. On the contrary, in the usual flat topologically trivial case, we show that the non-Abelian Skyrmions are only metastable solutions.

The paper is organized as follows. In the second section, the general setup in the usual flat metric with trivial topology is specified and the numerical solutions are described. In the third section, the low-energy action for the orientational moduli is introduced. In the fourth section, the setup to describe multi-Skyrmionic configurations at finite volume is analyzed and the issue of moduli condensation is discussed. In the fifth section some conclusions are drawn.

II. SETUP

In order to consider orientational moduli on Skyrmion configurations, we generalize the model introduced in [26]. We consider the action

$$S = \int d^4x(\mathcal{L}_{sk} + \mathcal{L}_{\chi} - \mathcal{L}_{\text{int}}) \tag{1}$$

where

$$\mathcal{L}_{sk} = \text{Tr}\left(\frac{\kappa}{4}(U^{-1}\partial_\mu U)^2 + \frac{\lambda}{4}[U^{-1}\partial_\mu U, U^{-1}\partial_\nu U] \times [U^{-1}\partial^\mu U, U^{-1}\partial^\nu U]\right), \tag{2}$$

$$\mathcal{L}_{\text{chi}} = \partial_\mu \chi^i \partial^\mu \chi^i, \tag{3}$$

$$\mathcal{L}_{\text{int}} = \gamma(Tr[U + U^{-1} - 2] + \Gamma)\chi^i\chi^i - \beta(\chi^i\chi^i)^2. \tag{4}$$

The Skyrme model possesses a conserved topological charge[1] which physically represents the baryon number (see [4,5]). Its integral expression is

$$W = -\frac{1}{24\pi^2}\int_{\{t=\text{const}\}} \text{tr}[(U^{-1}dU)^3], \tag{5}$$

where the integral is performed over $t = \text{const}$ hypersurfaces. Therefore, when $W \neq 0$, the corresponding configuration cannot be deformed continuously to the trivial vacua.

In the action we recognize $\mathcal{L}_{sk}$ as the usual Skyrme Lagrangian including the Skyrme term, $\mathcal{L}_{\chi}$ as the kinetic term of the triplet χ^i charged under the global non-Abelian group $O(3)$ and $\mathcal{L}_{\text{int}}$ as an interaction term. Just as per [26], the interaction term is designed to make the χ field condense on the core of the Skyrmion. We will take the dimensionless parameter $0 < \Gamma < 8$ and all other parameters as positive. The mass dimensions of the fields and parameters are $[U] = 0, [\chi] = 1, [\gamma] = [\kappa] = 2, [\beta] = [\lambda] = 0$. Our metric convention is $\eta_{\mu\nu} = (-,+,+,+)$ and the convention on the group generators is $t_i = i\sigma_i$. We use a spherical coordinate system and switch to the dimensionless units of $\rho = \sqrt{\kappa}r$ and $\tilde{\chi} = \chi/\sqrt{\kappa}$ (which we will adopt from here throughout).

We take the following *Ansatz* for our fields:

$$U = \cos(\alpha(\rho))\mathbb{I}_2 + \sin(\alpha(\rho))n_a t_a, \tag{6}$$

$$\chi^i = \tilde{\chi}(\rho)(0,0,1), \tag{7}$$

where $n_a = x_a/r$ and $\mathbb{I}_2$ is the two-dimensional identity matrix. Then the energy functional reduces to

$$\frac{E}{2\pi\sqrt{\kappa}} = \int_0^\infty d\rho\rho^2\left(\frac{(\sin\alpha)^2}{\rho^2} - \frac{2\lambda(\sin\alpha)^2(-1+\cos(2\alpha)-4\rho^2(\alpha'^2))}{\rho^4} + \frac{1}{2}\alpha'^2 + \frac{\gamma}{\kappa}(-4+\Gamma+4\cos\alpha)\tilde{\chi}^2 - \beta\tilde{\chi}^4 + \tilde{\chi}'^2\right), \tag{8}$$

[1]Mathematically, this charge is the winding number associated to the third homotopy class of maps from the three-dimensional sphere into $SU(2)$.

with $'$ denoting differentiation with respect to ρ. It can be easily checked that with the above *Ansatz* for the Skyrmion and for the χ field the equations of motion coincide with the equations obtained as stationary points of the above energy functional.

A. Vacuum structure

Assuming constant field profiles at infinity and minimizing the energy functional at leading order in $(1/\rho)$ we obtain the following equations:

$$\tilde{\chi}_{\rm vac}\sin\alpha_{\rm vac}=0, \tag{9}$$

$$\tilde{\chi}_{\rm vac}\left(\tilde{\chi}_{\rm vac}^2-\frac{\gamma}{2\beta\kappa}(-4+\Gamma+4\cos\alpha_{\rm vac})\right)=0. \tag{10}$$

These set of equations have solutions of the form

$$\tilde{\chi}_{\rm vac}=0, \qquad \alpha_{\rm vac}=C, \tag{11}$$

where $0\le C\le 2\pi$ is an arbitrary angular constant, or

$$\alpha_{\rm vac}=n\pi,$$
$$\tilde{\chi}_{\rm vac}=\pm\sqrt{\frac{\gamma}{2\beta\kappa}(-4+\Gamma+4(-1)^n)}, \tag{12}$$

where n is an integer. Since we are working with the condition $0<\Gamma<8$ (and all other parameters positive) then, for reality of $\tilde{\chi}_{\rm vac}$ we must disregard n odd and only consider even cases. For these cases the corresponding energies of the vacuum solutions are

$$\frac{E_1}{2\pi\sqrt{\kappa}}=0, \qquad \frac{E_2}{2\pi\sqrt{\kappa}}=\frac{\gamma^2\Gamma^2}{4|\beta|\kappa^2}. \tag{13}$$

One can fix the constant $C=0$, meaning the true vacuum is at $U=\mathbb{I}_2$ and $\tilde{\chi}=0$. Note that the two branches coalesce at $\Gamma=0$.

B. Energy minimization equations

The equations which minimize the energy functional reduce to the coupled set of ordinary differential equations (ODEs)

$$\alpha''+\frac{2\alpha'}{\rho}-\frac{\sin(2\alpha)}{\rho^2}-8\lambda\left[\frac{\sin(2\alpha)\sin(\alpha)^2}{\rho^4}-\frac{\sin(2\alpha)\alpha'^2}{\rho^2}-\frac{2(\sin\alpha)^2\alpha''}{\rho^2}\right]-\frac{4\gamma}{\kappa}\sin(\alpha)\tilde{\chi}^2=0, \tag{14}$$

$$\tilde{\chi}''+\frac{2\tilde{\chi}'}{\rho}-\frac{\gamma}{\kappa}(-4+4\cos(\alpha)+\Gamma)\tilde{\chi}+2\beta\tilde{\chi}^3=0. \tag{15}$$

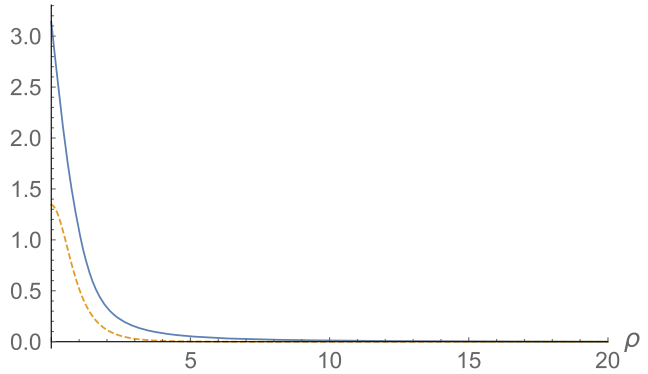

FIG. 1. Solution for $\gamma/\kappa=1$, $\beta=0.05$, $\lambda=1/8$ and $\Gamma=1$, solid line is α, dashed line is $\tilde{\chi}$.

The above equations must be solved numerically. In order to look for Skyrmion solutions we solve these equations with the following boundary conditions:

$$\alpha(0)=\pi, \qquad \tilde{\chi}'(0)=0, \tag{16}$$

$$\alpha(\infty)=0, \qquad \tilde{\chi}(\infty)=0. \tag{17}$$

Our numerical procedure is a second-order finite difference procedure with accuracy $\mathcal{O}(10^{-3})$. The solution is shown in Fig. 1.

C. Mass

In this section we will compare the mass of the solution with and without moduli. This gives an indication as to which solution is energetically preferred. The energy on our solution, with the parameters outlined in the figure, evaluates to

$$\frac{E}{2\pi\sqrt{\kappa}}=5.966, \tag{18}$$

while the energy of the $\tilde{\chi}=0$ solution is

$$\frac{E}{2\pi\sqrt{\kappa}}=5.804. \tag{19}$$

Clearly the solution with moduli is higher in energy than the normal Skyrmion. This result holds for the complete parameter range we have investigated for which our numerical procedure converged. In particular, the results for the masses diverge as γ/κ and/or β increases (for the parameters quoted in the solution, we found convergence up to $\beta=0.09$ and $\gamma/\kappa=2.625$). Both parameter changes increase the value of $\tilde{\chi}$ in the core. Therefore, it must be an unstable, or at most metastable, solution. This is in strong contrast to the case of vortices [29] or monopoles [31], where the presence of additional moduli is energetically preferred.

In the next section we will argue that the solution is metastable.

D. Stability

Since the energy of the solution with additional moduli is higher than the one without, we must check that the solution is not unstable.

Perturbing our solutions with perturbations of the form

$$\alpha = \alpha_0 + \alpha_p e^{-i\omega t},$$
$$\chi^i = (\tilde{\chi}_{1p} e^{-i\omega t}, \tilde{\chi}_{2p} e^{-i\omega t}, \tilde{\chi}_0 + \tilde{\chi}_{3p} e^{-i\omega t}) \tag{20}$$

where α_0 and $\tilde{\chi}_0$ are the background solutions obtained above and $\tilde{\chi}_{ip}$ is a perturbation of the χ field in the color direction i, we obtain the following set of coupled equations for the perturbations:

$$\begin{pmatrix} \Delta_1 & \Delta_\chi \\ \Delta_\alpha & \Delta_2 \end{pmatrix} \begin{pmatrix} \alpha_p \\ \tilde{\chi}_{3p} \end{pmatrix} = 0, \tag{21}$$

where, using the previously introduced dimensionless units and $\tilde{\omega} = \omega/\sqrt{\kappa}$, we have

$$\Delta_1 = V_{(1)} - \rho^2((\partial_\rho \Psi_{(1)})\partial_\rho + \Psi_{(1)}\partial_\rho^2), \tag{22}$$

$$\Delta_2 = V_{(2)} - \frac{1}{\rho}((\partial_\rho \Psi_{(2)})\partial_\rho + \Psi_{(2)}\partial_\rho^2), \tag{23}$$

and

$$V_{(1)} = -\rho^2(\rho^2 + 8\lambda)\tilde{\omega}^2 - 8\lambda\cos(4\alpha_0) + 4\frac{\gamma}{\kappa}\rho^4\cos(\alpha_0)\tilde{\chi}_0^2 + 2\cos(2\alpha_0)(4\lambda + \rho^2(1 + 4\lambda\tilde{\omega}^2) - 8\rho^2\lambda(\alpha_0'^2) - 16\rho^2\lambda\sin(2\alpha_0)\alpha_0'', \tag{24}$$

$$V_{(2)} = \rho\left(\frac{\gamma}{\kappa}(-4 + \Gamma) - \tilde{\omega}^2 + 4\frac{\gamma}{\kappa}\cos(\alpha_0) - 6\beta\tilde{\chi}_0{}^2\right), \tag{25}$$

$$\Psi_{(1)} = (\rho^2 + 8\lambda(1 - \cos(2\alpha_0))), \tag{26}$$

$$\Psi_{(2)} = \rho^2, \tag{27}$$

$$\Delta_\chi = 8\frac{\gamma}{\kappa}\rho^4\sin(\alpha_0)\tilde{\chi}_0, \tag{28}$$

$$\Delta_\alpha = -4\frac{\gamma}{\kappa}\rho\sin(\alpha_0)\tilde{\chi}_0. \tag{29}$$

The perturbations in the orthogonal colour directions decouple and obey the following equation:

$$\tilde{\chi}_{ip}'' + \frac{2}{\rho}\tilde{\chi}_{ip}' + \tilde{\chi}_{ip}(\gamma(4 - \Gamma - 4\cos(\alpha_0)) + \tilde{\omega}^2 + 2\beta\tilde{\chi}_0^2) = 0, \tag{30}$$

with $i = 1, 2$. We can put this equation in a convenient form by using the transformation $\tilde{\chi}_{ip} = \hat{\chi}_{ip}/\rho$ to obtain the Schrödinger equation

$$\hat{\chi}_{ip}'' + \hat{\chi}_{ip}(\gamma(4 - \Gamma - 4\cos(\alpha_0)) + \tilde{\omega}^2 + 2\beta\tilde{\chi}_0^2) = 0. \tag{31}$$

In order to proceed with the stability analysis we make a change of variables which simplifies the analysis of the coupled modes, we take

$$\alpha_p = Fu, \qquad \tilde{\chi}_p = Gv, \tag{32}$$

$$F = \frac{1}{\sqrt{\Psi_{(1)}}}, \qquad G = \frac{1}{\sqrt{\Psi_{(2)}}}, \tag{33}$$

where u and v are the new unknowns in the linearized equations. In terms of the new variables the linearized equations read

$$\Delta_\chi G v + V_{(1)}Fu - \rho^2[V_{(3)}u + \Psi_{(1)}F\partial_\rho^2 u] = 0, \tag{34}$$

$$\Delta_\alpha F u + V_{(2)}Gv - \frac{1}{\rho}[V_{(4)}v + \Psi_{(2)}G\partial_\rho^2 v] = 0, \tag{35}$$

$$V_{(3)} = [(\partial_\rho \Psi_{(1)})(\partial_\rho F) + \Psi_{(1)}\partial_\rho^2 F], \tag{36}$$

$$V_{(4)} = [(\partial_\rho \Psi_{(2)})(\partial_\rho G) + \Psi_{(2)}\partial_\rho^2 G]. \tag{37}$$

Through this change of variables, the linearized system for the perturbations equations (34) and (35) has been reduced to a system of coupled Schrödinger equations.

Our strategy to analyze the stability issue is the following: we find the lowest energy normalizable solution of the coupled Schrödinger equations (36)–(37). This solution will have normalizable profiles for both u and v components and a minimum number of total nodes. The solution is found by varying $\tilde{\omega}^2$. If $\tilde{\omega}$ is such that $\tilde{\omega}^2 < 0$ this indicates an instability of the solution. We find numerically that $\tilde{\omega}^2 \approx 1.1 > 0$, indicating that our solution is stable. For the perturbation modes in the orthogonal color directions an analogous analysis of Eq. (31) yields $\tilde{\omega}^2 \approx 8 > 0$.

Clearly, since the energy of our solution is higher than that with $\tilde{\chi} = 0$, our solution is actually metastable.

III. LOW-ENERGY THEORY OF ORIENTATIONAL MODULI

Standard quantization of the $SU(2)$ Skyrmion involves six moduli: three translations of the Skyrmion center and three space-flavor locked rotations (see [33] for a review). The quantum mechanical Hamiltonian of these moduli is

$$\mathcal{H} = M_{sk} + \frac{\vec{p}^2}{2M_{sk}} + \frac{1}{2I_{sk}} J(J+1), \tag{38}$$

where J is a spin (or equivalently isospin) label. In the above $I_{sk} \approx 26 \times \frac{51\pi\lambda^{3/2}}{3\sqrt{\kappa}}$ [33]. The presence of additional orientational moduli will give an extra isospin quantum number. To see this we parametrize the moduli field $\tilde{\chi}$ as

$$\chi^i = \tilde{\chi}(\rho) S^i(t), \tag{39}$$

with S^i a unit vector satisfying $S^i S^i = 1$. Then inserting this parametrization into Eq. (1) we obtain the low-energy effective action

$$S_{le} = \frac{I_1}{2} \int dt \dot{S}^i \dot{S}^i, \qquad S^i S^i = 1. \tag{40}$$

On symmetry grounds this is simply the $CP(1)$ nonlinear sigma model which results from the breaking pattern $O(3) \to U(1)$. The constant I_1, which plays the role of the moment of inertia, evaluates numerically to

$$\frac{I_1\sqrt{\kappa}}{4\pi} = \int_0^\infty \rho^2 \tilde{\chi}^2 d\rho = 0.372. \tag{41}$$

Quantization of this action follows the quantization of a rigid top (see [31]). It results in energy levels of the form

$$E_s = \frac{1}{2I_1} s(s+1), \tag{42}$$

with degeneracy $2s+1$ and spherical harmonic eigenfunctions.

As a curious possibility, in all the special cases in which

$$\frac{I_{sk}}{I_1} = \frac{p}{q}, \qquad p, \quad q \in \mathbb{N}, \tag{43}$$

the eigenvalues of the Hamiltonian of the moduli read

$$\mathcal{H} = M_{sk} + \frac{\vec{p}^2}{2M_{sk}} + \frac{1}{2qI_{sk}} [qJ(J+1) + ps(s+1)].$$

Therefore, in this case, the discrete part of the spectrum would be determined by the integer number

$$N(J,s) = qJ(J+1) + ps(s+1).$$

It is easy to see that generically (once p and q are fixed) there is a greater degeneracy of the energy states. Physically, an increase in degeneracy of energy levels is associated with an enhancement of the original symmetry. However, there is no obvious reason why Eq. (43) should be satisfied as this depends numerically on the parameters of our system.

IV. MULTI-SKYRMIONS IN TUBULAR TOPOLOGY

One of the key properties of the hedgehog *Ansatz* for $SU(2)$-valued scalar fields is that it reduces a matrix system of coupled nonlinear partial differential equations (PDEs) to a single scalar nonlinear ODE for the soliton profile keeping alive, at the same time, the corresponding topological features of the matrix-valued field. This property is important in all contexts in which such *Ansätze* are used, from nonlinear sigma models to the Skyrme model (see [2] for detailed reviews). Obviously, even when the scalar equation for the soliton profile is not solvable analytically, the reduction of a matrix system of coupled PDEs to a single ODE is a huge technical advantage both theoretically and numerically. This property becomes even more important in the cases in which multi-Skyrmionic configurations are considered. In [16,18], using the formalism developed in Refs. [12–14], the matrix valued field equations of the four-dimensional Skyrme sigma model have been reduced to a single scalar ODE for the soliton profile in a sector of arbitrary topological charge (and in such a way as to consider finite-volume effects as well). These are the basic technical results which we use here to construct non-Abelian multi-Skyrmion configurations.

Therefore, we change to a different topology with metric given by

$$ds^2 = -dt^2 + dr^2 + R^2(d\theta^2 + (\sin\theta)^2 d\psi^2). \tag{44}$$

This is the metric for the Cartesian product space $\mathcal{R}^{(1,1)} \times S^2$.

The usefulness of this geometry lies in the fact that it allows one to study finite-volume effects (such effects usually make both numerical and analytical studies very complicated; see [11]) keeping at the same time the advantages coming from the symmetries of the hedgehog *Ansatz*. It describes three-dimensional cylinders whose sections are two-dimensional spheres. Consequently, the parameter R plays the role of the diameter of the transverse sections of the tube. From the computational point of view, the above choice of the metric is convenient since the radial variable r which usually appears in front of the angles in the Minkowski metric is replaced by a constant parameter (namely, R). This leads to considerable simplifications, as the following analysis will prove. There is a price to pay of course as the metric is curved. However, as the curvature of this metric is proportional to $\frac{1}{R^2}$ one can easily consider a flat limit by taking R large. In the case of the Skyrme model, large means that R should be much larger than 1 fm.

It is possible to be more precise about the effects of the local curvature of the above metric. The Skyrme model is the leading approximation in the large-$\mathbf{N}$ limit of the low-energy action of QCD [4]; however, subleading corrections in $1/\mathbf{N}$ do appear. Thus, from the practical point of view, if

one takes $R \sim 100$ fm the effects of the curvature are already much smaller than other corrections to the Skyrme model arising from QCD in the large-**N** expansion.

Therefore, the above metric can be considered as a "regulator." It is worth emphasizing that this trick is also extremely useful when dealing with 't Hooft-Polyakov BPS monopoles [34]. We also make one other different consideration: in this topology we work with values of $\beta < 0$ for reasons which will soon be explained. All other parameters are the same as before.

An important remark about the above geometry is in order. One may wonder whether the usual identification of Skrmions with fermions still holds on the chosen curved geometry. In Ref. [35] the argument of [36] has been generalized to curved orientable compact spaces. As the spatial sections of the chosen geometry are orientable and compact, we can claim that the third homotopy class is the baryon charge in the present case as well. This is a useful observation since, in the above geometry, there are topological excitations in the Skyrme model with topological charges different from the baryon charge (see for instance [14]). Such excitations with vanishing baryon charge should be considered as topological excitations of the pionic sector. On the other hand, the multi-Skyrmions which will be constructed here cannot decay into these excitation of the pionic sector as the baryon charge is conserved.

In the new topology the energy (under the same *Ansatz*) becomes

$$\frac{E}{2\pi\sqrt{\kappa}} = \int_0^L d\rho \Bigg((\sin\alpha)^2 - \frac{2\lambda(\sin\alpha)^2(-1+\cos(2\alpha)-4R^2\kappa(\alpha'^2))}{\kappa R^2} + \frac{\kappa R^2}{2}(\alpha'^2) + \gamma R^2(-4+\Gamma+4\cos\alpha)\tilde{\chi}^2 + |\beta|\kappa R^2\tilde{\chi}^4 + \kappa R^2(\tilde{\chi}'^2) \Bigg), \tag{45}$$

which is minimized by solving the equations

$$\left(1+\frac{16\lambda(\sin\alpha)^2}{\kappa R^2}\right)\alpha'' - \frac{\sin(2\alpha)}{\kappa R^2}\left(1-8\lambda\left(\alpha'^2-\frac{(\sin\alpha)^2}{\kappa R^2}\right)\right) - \frac{4\gamma}{\kappa}(\sin\alpha)\tilde{\chi}^2 = 0, \tag{46}$$

$$\frac{\gamma}{\kappa}(4(-1+\cos\alpha)+\Gamma)\tilde{\chi} + 2|\beta|\tilde{\chi}^3 - \tilde{\chi}'' = 0. \tag{47}$$

Also in this case the full field equations of motion are equivalent to the above coupled system of equations corresponding to the stationary condition for the energy functional.

Note that this finite-volume topology has important consequences on the energetic considerations. First, there is no origin in this geometry since $\rho = 0$ is simply a convention of where to begin the length of the tube. This implies that one can obtain energetically finite solutions without vanishing derivatives there. Also, solutions have finite energy even though they do not vanish at infinity, precisely because we consider a geometry with finite length. In particular, since $\beta < 0$, the lowest-energy vacuum solution of Eq. (45) has [see Eq. (13)]

$$\alpha = (2n+1)\pi, \qquad \tilde{\chi}_{\rm vac} = \pm\sqrt{\frac{\gamma}{2|\beta|\kappa}(8-\Gamma)}, \tag{48}$$

with energy

$$E_{\rm vac} = -\frac{\gamma^2}{4|\beta|\kappa^2}(-8+\Gamma)^2. \tag{49}$$

The important point is that solutions inside the finite geometry which do not tend to the vacua at the extrema still have finite energy and, consequently, still correspond to solutions with normalizable orientational moduli, as we will shortly show. Therefore, in the remainder of this section, when dealing with energetic considerations, we will not include this constant shift in vacuum energy.

For the Skyrme *Ansatz* in Eq. (6) the baryon number in Eq. (5) reduces to

$$W = \frac{2}{\pi}\int_{\alpha(0)}^{\alpha(L)} \sin^2\alpha d\alpha,$$

L being the length of the tube. Thus, the baryon number depends exclusively on the boundary conditions for the Skyrmion profile α. In particular

$$\alpha(L) - \alpha(0) = n\pi \Rightarrow W = n.$$

Actually, out of all the allowed integer values of n (which denotes the number of Skyrmions), we can categorize the families of solutions between two possibilities (namely, n even and n odd) which correspond to periodic and antiperiodic boundary conditions for the Skyrme field U in Eq. (6),

$$n \text{ even} \Rightarrow U(0) = U(L),$$
$$n \text{ odd} \Rightarrow U(0) = -U(L).$$

A. Multi-Skyrmion solutions and energy considerations

Here we present some solutions to the above equations. To find Skyrmion solutions of baryon number n we use boundary conditions of the form (see explanation above)

$$\alpha(0) = 0, \qquad \tilde{\chi}'(0) = 0, \tag{50}$$

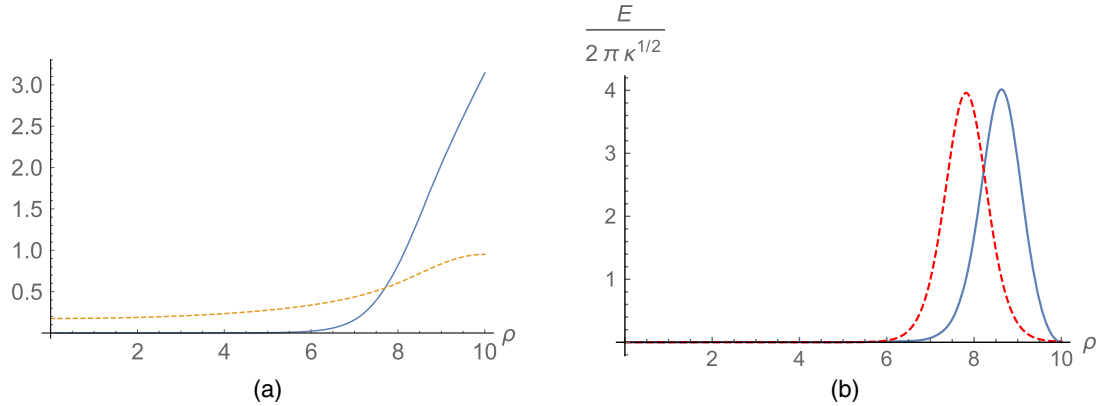

FIG. 2. Plot at $\lambda = 1/8$, $|\beta| = 0.4$, $\Gamma = 0$, $\gamma/\kappa = 1/4$ and $\sqrt{\kappa}R = 0.27$. (a) The solid line is the profile α and the dashed line is the profile χ. (b) The energy plot with (blue plot) and without (dashed red the plot) any moduli.

$$\alpha(L) = n\pi, \qquad \tilde{\chi}'(L) = 0, \tag{51}$$

where L is the dimensionless length of the tube we are placing the Skyrmions in and n the number of them. Note that we can choose Neumann-type boundary conditions for $\tilde{\chi}$ at both extremities of the geometry since it is both bounded in length and has no origin.

The solution corresponding to a single Skyrmion inside the tube is shown in Fig. 2, alongside its energy compared to the case without any moduli. The multi-Skyrmion solutions are shown in Fig. 3. In Fig. 1 we calculate the dimensionless energies of the corresponding solutions with their percentage differences defined by

$$\%\,\text{diff} = \frac{E_{sk} - E_{\chi}}{E_{sk}} \times 100. \tag{52}$$

We see that in finite volume, and in this particular topology, solutions with orientational moduli are energetically preferred over solutions without. This is in sharp contrast to our findings in flat space (described in Sec. II). For fixed length L of the tube, this difference grows with the number of Skyrmions up until $n = 3$, at which point it seems to drop. We find using our numerical procedure that there is a narrow range of parameters for which, for the same values of the parameters, convergence is seen up to $n = 5$. Therefore, the results shown in Table I are specific to a window of parameters with negligible variation from those quoted and may not necessarily follow a similar pattern generically.

Furthermore, for fixed L, as seen by the energy plots, the presence of additional orientational moduli serves to decrease the Skyrmion repulsion, decreasing the separation between each Skyrmion [see Fig. 3(b)]. This effect is not *a priori* surprising. The presence of an additional bosonic scalar degree of freedom within the tube provides an attractive force between Skyrmions which contrasts their repulsion. The χ field is in this way partially screening the repulsive force.

The decrease of the repulsion energy would be even larger if one would consider moduli which can condense separately on each elementary Skyrmion [instead of being rigid, as implied by the *Ansatz* in Eq. (39)]. However this would complicate the numerical analysis considerably as the present system of coupled ODEs would become a system of nonlinear coupled PDEs (see discussion below). We hope to come back to this issue in a future publication.

B. Low-energy theory of orientational moduli

The low-energy theory of the additional orientational moduli follows closely that derived in Sec. III. Even though the solutions represent multi-Skyrmions there still remains one explicit zero mode corresponding to the equal global rotation of all the Skyrmions inside the global group. This is seen precisely as per the flat case, taking $\tilde{\chi}$ as

$$\chi^i = \tilde{\chi}(\rho) S^i(t), \tag{53}$$

with S^i a unit vector satisfying $S^i S^i = 1$. Then, inserting this parametrization into Eq. (1), we obtain the low-energy effective action

$$S_{le} = \frac{I_2}{2} \int dt \dot{S}^i \dot{S}^i, \qquad S^i S^i = 1. \tag{54}$$

The constant I_2 now evaluates to

$$\frac{I_2\sqrt{\kappa}}{4\pi} = \kappa R^2 \int_0^L \tilde{\chi}^2 d\rho = 1.06. \tag{55}$$

The presence of the extra moduli tends to decrease the repulsive interactions between the elementary Skyrmions; hence, it is natural to wonder whether one can decrease this even further with a less rigid moduli configuration. The natural guess is that if the moduli could condense on each elementary Skyrmion independently, then the decrease of the repulsive interactions would be even larger. However,

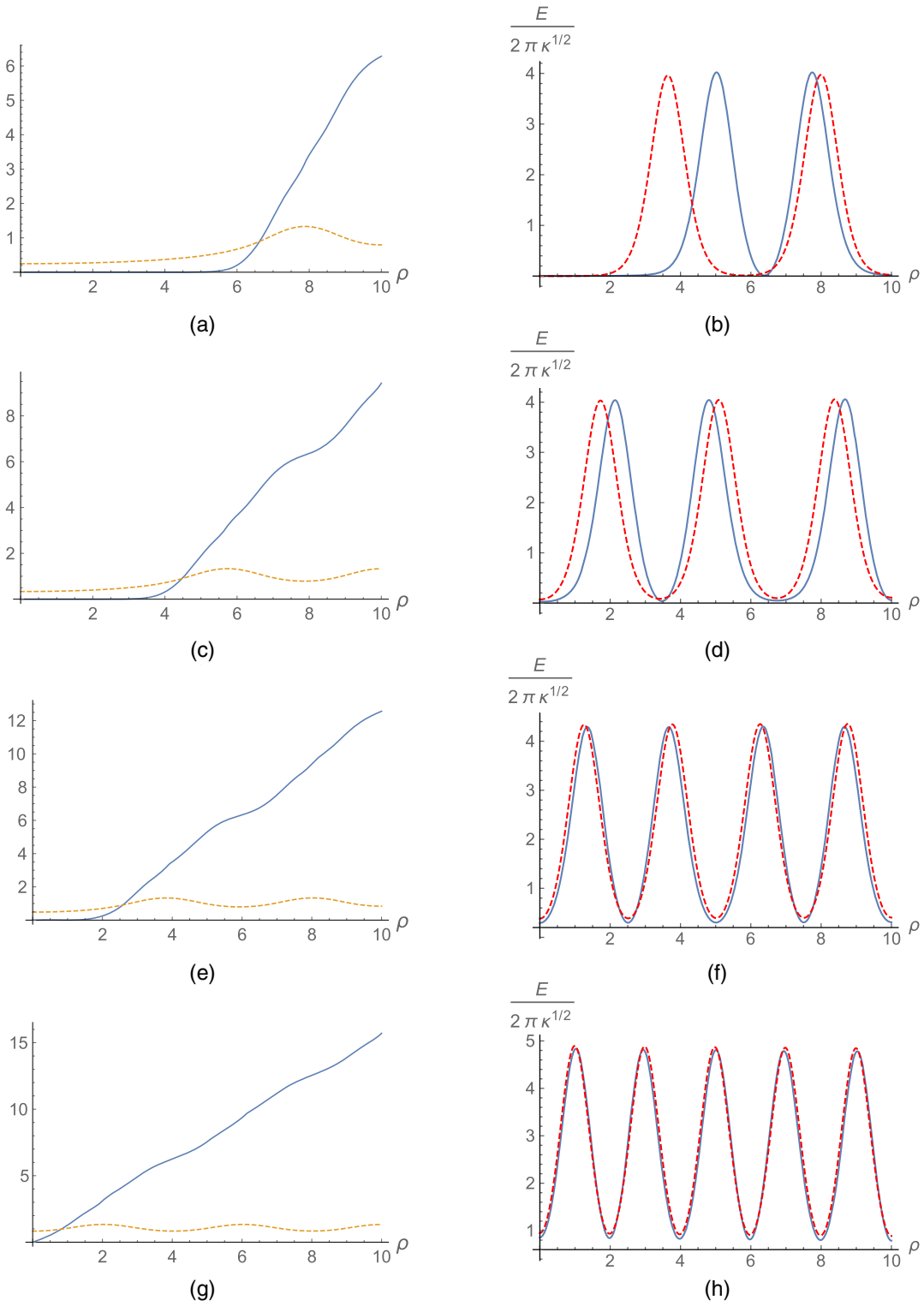

FIG. 3. All plots at $\lambda = 1/8$, $|\beta| = 0.4$, $\Gamma = 0$, $\gamma/\kappa = 1/4$ and $\sqrt{\kappa}R = 0.27$. (a) The solid line is the profile α and the dashed line is the profile χ in the sector with baryon number 2. (b) The energy plot with (blue plot) and without (dashed red the plot) any moduli in the sector with baryon number 2. (c) The solid line is the profile α and the dashed line is the profile χ in the sector with baryon number 3. (d) The energy plot with (blue plot) and without (dashed red the plot) any moduli in the sector with baryon number 3. (e) The solid line is the profile α and the dashed line is the profile χ in the sector with baryon number 4. (f) The energy plot with (blue plot) and without (dashed red the plot) any moduli in the sector with baryon number 4. (g) The solid line is the profile α and the dashed line is the profile χ in the sector with baryon number 5. (h) The energy plot with (blue plot) and without (dashed red the plot) any moduli in the sector with baryon number 5.

TABLE I. Comparisons of the Skyrmions energies without (first column) and with (second column) extra moduli with Skyrmion number from 1 to 5. In the third column one can read the corresponding normalized energy difference.

n	E of pure Skyrmions	E of Skyrmions with $\tilde{\chi}$	% difference
1	4.92	4.77	3.05
2	9.85	9.53	3.24
3	14.9	14.3	4.03
4	20.6	19.8	3.88
5	27.2	26.4	2.94

an *Ansatz* of the form in Eq. (39) is not suitable to achieve this goal. The reason is that the factorized expression $\chi^i = \tilde{\chi}(\rho)S^i(t)$ implies that the extra isospin number related to the unit vector $S^i(t)$ is the same in any point of the tube. We would like to describe a situation in which the orientation of the unit vector $S^i(t)$ depends on the position of the tube and, in particular, is able to distinguish the elementary Skyrmions. In this respect, a reasonable *Ansatz* is

$$\chi^i_L = \tilde{\chi}(\rho)S^i(t,\rho),$$

in order to be able to have a different S^i on each elementary Skyrmion living within such a finite-volume region. However, such an *Ansatz* would lead to a system of coupled PDEs and would complicate the numerical analysis. We hope to come back to this interesting issue in a future publication.

We can however make some intuitive progress by considering a dramatic simplification. If we assume that the $\tilde{\chi}$ field is approximately localized on each Skyrmion in the tube then we may consider an *Ansatz* of the form

$$\chi(\rho)^i \approx \sum_{j=1}^{n} \chi_j \Pi(\alpha_j \delta(\rho-\rho_j)) S^i_{\rho_j}(t), \tag{56}$$

where $\chi_j\Pi(\alpha_j\delta(\rho-\rho_j))$ is a rectangular function of width α_j and height χ_j localized on each Skyrmion center ρ_j, to which we assign an orientational moduli vector $S^i_{\rho_j}(t)$. The *Ansatz* represents a total function $\chi(\rho)^i$ in the length of the tube as the sum of each individual Skyrmion contribution, crudely approximated by a step function. In this case we can immediately observe how moduli interactions arise; consider for example the potential term

$$\chi^i\chi^i \approx \sum_{k=1}^{n}\sum_{j=1}^{n} \chi_j\chi_k S^i_{\rho_j}(t)S^i_{\rho_k}(t)\Pi(\alpha_j\delta(\rho-\rho_j))\Pi(\alpha_k\delta(\rho-\rho_k)) \tag{57}$$

Then, in the limit in which the rectangular functions have infinitesimal width $|\rho_i-\rho_j| \gg |\alpha_i-\alpha_j|$ (the step function tend to delta functions), so that each Skyrmion modulus is perfectly localized, this expression is independent of the moduli since the condition $S^i_j S^i_j = 1$ applies (no sum over j). However, if the moduli overlap within a finite region, $|\rho_i-\rho_j| \approx |\alpha_i-\alpha_j|$, then terms with $S^i_j S^i_k$ with $j \neq k$ are nonvanishing. These kind of terms are clearly present in the solutions we observe numerically in Fig. 3 where $\tilde{\chi}(\rho)$ is dispersed and nowhere vanishing within the tube. Through these interactions the moduli are lifted and become quasimoduli. The only remaining true modulus is the global rotation discussed at the beginning of this section.

C. Large-R flat limit

As already remarked, the technical advantage of the geometry in Eq. (44) lies in the fact that it allows one to keep the symmetries of the hedgehog *Ansatz* without losing information about the finiteness of the volume where the elementary Skyrmions live. *Per se* this provides a very simple framework to analyze the issue of (orientational) moduli in the presence of configurations of arbitrary baryon number. Such tube-shaped regions are however not flat as the curvature of this metric is proportional to $\frac{1}{R^2}$.

As far as the local effects of the curvature are concerned, they can be considered small when they are negligible with respect to the corrections which the Skyrme model receives in the large-**N** expansion of QCD [4]. This happens already when $R \sim 100$ fm. However, one can take a formal large $\sqrt{\kappa}R$ limit directly in the field equations (46)–(47) which, in the leading order of such expansion, read

$$\alpha'' - \frac{4\gamma}{\kappa}(\sin\alpha)\tilde{\chi}^2 = 0, \tag{58}$$

$$\frac{\gamma}{\kappa}(4(-1+\cos\alpha)+\Gamma)\tilde{\chi} + 2|\beta|\tilde{\chi}^3 - \tilde{\chi}'' = 0. \tag{59}$$

The above system is considerably simpler but still nontrivial due to the nonlinear interactions which are still present. Solving the above equations with boundary conditions of arbitrary baryon number [those of Eqs. (50) and (51)] can be thought to represent, in the flat case, multi-Skyrmion configurations constrained to live within flat tubes whose sections have dimension much bigger than 1 fm. Each elementary Skyrmion belonging to these multi-Skyrmionic configurations is very well localized in the direction of the axis of the tube (namely, the energy density profile in the large-R limit looks almost like the superposition of many nonoverlapping peaks, one for each elementary Skyrmion). On the other hand, in the spatial directions orthogonal to the axis

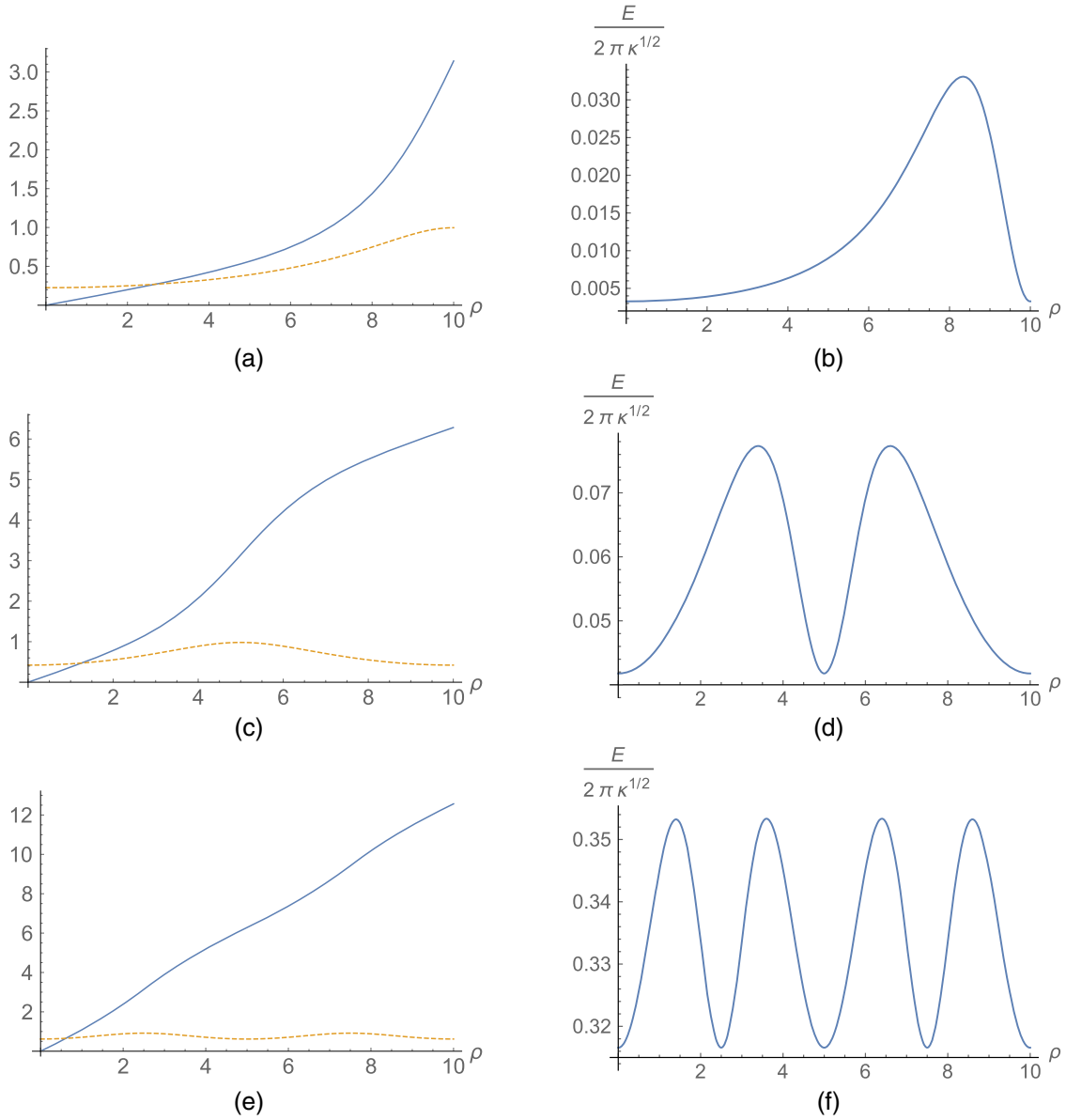

FIG. 4. All plots at $\lambda = 1/8$, $|\beta| = 0.4$, $\Gamma = 0$, $\gamma/\kappa = 1/4$. (a) The solid line is the profile α and the dashed line is the profile χ in the sector with baryon number 1 in the large-R limit. (b) The energy plot in the sector with Baryon number 1 in the large-R limit. (c) The solid line is the profile α and the dashed line is the profile χ in the sector with baryon number 2 in the large-R limit. (d) The energy plot in the sector with Baryon number 2 in the large-R limit. (e) The solid line is the profile α and the dashed line is the profile χ in the sector with baryon number 4 in the large-R limit. (f) The energy plot in the sector with Baryon number 4 in the large-R limit.

of the tube, the Skyrmions are homogeneous (in other words, the energy density profile does not depend on the coordinates transverse to the axis). Solutions of this form are shown in Fig. 4. Note that in this case the solution with $\tilde{\chi} = 0$ is just the linear function $\alpha = \frac{n\pi}{L}\rho$ which reduces the energy to an n-dependent constant.

An interesting issue on which we hope to come back in a future publication is to develop in a systematic way the large-R expansion in which (a suitable "adimensionalized" version of) $\frac{1}{R^2}$ would play the role of small parameter.

V. CONCLUSIONS

In the present paper, combining the construction of analytic multi-Skyrmionic configurations with the recent approach to the analysis of orientational moduli [26], we analyzed how extra orientational moduli affect the properties of multi-Skyrmionic configurations of the four-dimensional Skyrme model. This analysis sheds light on the peculiar behavior of orientational moduli when multi-solitonic configurations are present. It reveals interesting novel features. First of all, when considering finite geometry, the orientational moduli tend to decrease the

repulsive interactions among elementary $SU(2)$ Skyrmions (however, this effect decreases with the increase of the baryon number). Moreover, in the case of a single Skyrmion, the appearance of moduli is energetically favorable if finite-volume effects are present; otherwise, in the usual flat topologically trivial case, it is not.

ACKNOWLEDGMENTS

This work has been funded by Fondecyt Grants No. 1160137 and No. 3140122. The Centro de Estudios Científicos (CECs) is funded by the Chilean Government through the Centers of Excellence Base Financing Program of Conicyt.

[1] T. H. R. Skyrme, Proc. R. Soc. A **260**, 127 (1961); **262**, 237 (1961); Nucl. Phys. **31**, 556 (1962).
[2] N. Manton and P. Sutcliffe, *Topological Solitons* (Cambridge University Press, Cambridge, England, 2007).
[3] D. Finkelstein and J. Rubinstein, J. Math. Phys. (N.Y.) **9**, 1762 (1968).
[4] E. Witten, Nucl. Phys. **B160**, 57 (1979); **B223**, 422 (1983); **B223**, 433 (1983).
[5] A. P. Balachandran, F. Lizzi, and G. Sparano, Nucl. Phys. **B263**, 608 (1986).
[6] G. S. Adkins, C. R. Nappi, and E. Witten, Nucl. Phys. **B228**, 552 (1983).
[7] E. Guadagnini, Nucl. Phys. **B236**, 35 (1984).
[8] A. P. Balachandran, H. Gomm, and R. D. Sorkin, Nucl. Phys. **B281**, 573 (1987).
[9] A. P. Balachandran, A. Barducci, F. Lizzi, V. G. J. Rodgers, and A. Stern, Phys. Rev. Lett. **52**, 887 (1984).
[10] A. P. Balachandran, F. Lizzi, V. G. J. Rodgers, and A. Stern, Nucl. Phys. **B256**, 525 (1985).
[11] I. Klebanov, Nucl. Phys. **B262**, 133 (1985).
[12] F. Canfora and P. Salgado-Rebolledo, Phys. Rev. D **87**, 045023 (2013).
[13] F. Canfora and H. Maeda, Phys. Rev. D **87**, 084049 (2013).
[14] F. Canfora, Phys. Rev. D **88**, 065028 (2013).
[15] S. Chen, Y. Li, and Y. Yang, Phys. Rev. D **89**, 025007 (2014).
[16] F. Canfora, F. Correa, and J. Zanelli, Phys. Rev. D **90**, 085002 (2014).
[17] L. Bratek, Phys. Rev. D **78**, 025019 (2008).
[18] F. Canfora, M. Di Mauro, M. A. Kurkov, and A. Naddeo, Eur. Phys. J. C **75**, 443 (2015).
[19] E. Ayon-Beato, F. Canfora, and J. Zanelli, Phys. Lett. B **752**, 201 (2016).
[20] G. 't Hooft, Nucl. Phys. **B190**, 455 (1981); S. Mandelstam, Phys. Rep. **23**, 245 (1976).
[21] A. Hanany and D. Tong, J. High Energy Phys. 07 (2003) 037.
[22] R. Auzzi, S. Bolognesi, J. Evslin, K. Konishi, and A. Yung, Nucl. Phys. **B673**, 187 (2003).
[23] M. Shifman and A. Yung, Phys. Rev. D **70**, 045004 (2004).
[24] A. Hanany and D. Tong, J. High Energy Phys. 04 (2004) 066.
[25] E. Witten, Nucl. Phys. **B249**, 557 (1985).
[26] M. Shifman, Phys. Rev. D **87**, 025025 (2013).
[27] G. Tallarita, Phys. Rev. D **93**, 066011 (2016).
[28] M. Kobayashi, E. Nakano, and M. Nitta, J. High Energy Phys. 06 (2014) 130.
[29] M. Shifman, G. Tallarita, and A. Yung, Int. J. Mod. Phys. A **29**, 1450062 (2014).
[30] A. J. Peterson, M. Shifman, and G. Tallarita, Ann. Phys. (Amsterdam) **353**, 48 (2015).
[31] M. Shifman, G. Tallarita, and A. Yung, Phys. Rev. D **91**, 105026 (2015).
[32] A. J. Peterson, M. Shifman, and G. Tallarita, Ann. Phys. (Amsterdam) **363**, 515 (2015).
[33] M. Shifman, *Advanced Topics in Quantum Field Theory: A Lecture Course* (Cambridge University Press, Cambridge, England, 2012).
[34] F. Canfora and G. Tallarita, J. High Energy Phys. 09 (2014) 136; Phys. Rev. D **91**, 085033 (2015).
[35] D. Auckly and J. M. Speight, Commun. Math. Phys. **263**, 173 (2006).
[36] D. Giulini, Mod. Phys. Lett. A **08**, 1917 (1993).